



H-RN, a novel antiangiogenic peptide derived from hepatocyte growth factor inhibits inflammation in vitro and in vivo through PI3K/AKT/IKK/NF- κ B signal pathway



Lili Wang^{a,b}, Yan Xu^{a,b}, Qi Yu^{a,b}, Qiao Sun^{a,b}, Yi Xu^{a,b}, Qing Gu^{a,b}, Xun Xu^{a,b,*}

^a Department of Ophthalmology, Shanghai First People's Hospital, Shanghai Jiaotong University, No. 100, Haining Road, Shanghai, People's Republic of China

^b Shanghai Key Laboratory of Fundus Disease, No. 100, Haining Road, Shanghai, People's Republic of China

ARTICLE INFO

Article history:

Received 22 January 2014

Received in revised form 25 February 2014

Accepted 27 February 2014

Available online 11 March 2014

Chemical compounds studied in this article:

Dexamethasone sodium phosphate

(PubChem CID: 16961)

Lipopolysaccharide (PubChem CID:

53481793)

Keywords:

Peptide

Anti-inflammation

Endotoxin-induced uveitis (EIU)

Experimental autoimmune uveitis (EAU)

Nuclear factor (NF)- κ B

ABSTRACT

H-RN, a novel antiangiogenic peptide derived from the kringle 1 domain of hepatocyte growth factor (HGF), consists of the sequence RNPRGEEGPW (molecular weight: 1254.34 Da). Emerging evidence indicates that HGF and the kringle domain exhibit anti-inflammatory effects in inflammatory diseases. In the present study, we assessed the anti-inflammatory effect of H-RN in models of experimental ocular inflammation, including endotoxin-induced uveitis (EIU) and experimental autoimmune uveitis (EAU). The results demonstrated that intravitreal treatment of H-RN concentration-dependently suppressed clinical manifestation, inhibited ocular inflammatory cytokine production and improved histopathologic scores. Moreover, H-RN attenuated the LPS-induced mRNA and protein expression of tumor necrosis factor (TNF)- α and interleukin (IL)-6 in RAW 264.7 cells and inhibited cell chemotactic migration toward LPS. We also demonstrated that H-RN suppressed TNF- α -induced adhesion molecule expression in HUVECs, including ICAM-1, VCAM-1 and E-selectin, which contributed to its suppressive effect on adherence of U937 cells to endothelial cells. We also demonstrated the possible anti-inflammation mechanism of H-RN. Western blot and immunofluorescence staining analyses revealed that H-RN significantly suppressed LPS-induced phosphorylation of nuclear factor (NF)- κ B-p65 at Ser276. Based on examination of upstream pathways, we found that H-RN inhibited PI3K-p85 and AKT^{Ser473} phosphorylation, which may result in the attenuation of LPS-induced IKK complex activation and I κ B degradation. Thus, our studies suggest that the 11-amino-acid peptide H-RN exhibits anti-inflammatory effects in vitro and in vivo and may represent a promising candidate for ocular inflammatory diseases.

© 2014 Elsevier Inc. All rights reserved.

1. Introduction

Ocular angiogenic diseases, such as age-related macular degeneration and diabetic retinopathy, as well as inflammatory diseases, including uveitis, are sight-threatening diseases with important socioeconomic impacts [1,2]. Angiogenesis and inflammation are closely related in many biologic processes. Neovascularization accompanies inflammatory disease, including neovascular ocular diseases, rheumatoid arthritis and granulomatous diseases; in such cases, neovascularization may act to sustain inflammation, as new capillaries facilitate leukocyte entry into inflammatory lesions [3,4]. However, mediators such as tumor

necrosis factor (TNF)- α can induce inflammatory responses that lead to angiogenesis in vitro and in vivo [5,6].

Hepatocyte growth factor (HGF) was found to be a potent stimulator of new vessel formation and an important angiogenic factor in vascular retinopathies [7,8]. HGF was also demonstrated to suppress inflammation by inhibiting multiple pathophysiological processes involved in the inflammatory response, such as targeting inflamed microvascular endothelial cells and diminishing expression of several adhesion molecules [9]. The kringle domain, including HGF kringle 1 (HGF K1), was reported to exhibit antiangiogenic, antitumor and anti-inflammatory effects [10–14].

Previously, we identified a novel peptide, H-RN, derived from the HGF K1, and demonstrated its antiangiogenic activity in vitro and in vivo and its stability in aqueous solutions [15,16]. H-RN is composed of the 11 amino acid sequence RNPRGEEGPW (molecular weight: 1254.34 Da); its structure is presented in

* Corresponding author.

E-mail address: drxuxun@126.com (X. Xu).



Fig. 1. The peptide derived from the NK2 fragment of human HGF (Protein Data Bank accession no. 3HN4). The sequence of peptide H-RN was demonstrated in sticks mode in magenta, and the other part of the NK2 fragment of human HGF was represented in catoon form in wheat, shown with the PyMOL Molecular Graphic system (Delano Scientific).

Fig. 1. Due to the importance of inflammation in the process of neovascularization, we investigated anti-inflammatory effect of H-RN in cells and in experimental intraocular inflammation models. Because of the advantages of peptides, our study may lead to the discovery of new biological functions of H-RN and facilitate the development of potential therapies for ocular inflammatory diseases, including uveitis.

2. Materials and methods

2.1. Preparation of peptides

The peptide H-RN, a scrambled peptide H-GP (GPERWRGPNGE, molecular weight 1254.34 Da) as a negative control, fluorescein isothiocyanate (FITC)-labeled H-RN (FITC-RNPRGEEGPPW, molecular weight 1756.82 Da) and an interphotoreceptor retinoid-binding protein (IRBP) peptide spanning amino acid residues 1169–1191 (IRBP1169–1191, PTARSVGAADGSSWEGVGVDPV, R16) were synthesized and purified via solid-phase peptide synthesis using an automatic peptide synthesizer (Symphony; Protein Technologies, Tucson, AZ, USA) by ChinaPeptides Co., Ltd. (Shanghai, China).

2.2. Animals

Male Wistar rats (6–8 weeks old) procured from the Shanghai Laboratory Animal Center of the Chinese Academy of Sciences and female Lewis rats (6–8 weeks old) purchased from Vital River Laboratory Animal Technology Co., Ltd. (Beijing, China) were maintained in SPF conditions for one week prior to experimentation. Food and water were provided ad libitum. All animal experiments were in accordance with the ARVO Statement for the Use of Animals in Ophthalmic and Vision Research.

2.3. Endotoxin-induced uveitis (EIU)

2.3.1. EIU induction and treatment

EIU was induced via a single footpad injection of 100 μ l sterile pyrogen-free saline containing 200 μ g lipopolysaccharide (LPS) from *Escherichia coli*, o55:B5 (Sigma, St. Louis, MO, USA). The control group received the same volume of sterilized saline. Wistar rats from the various groups were intravitreally injected into both eyes with PBS, H-RN (1, 5 or 10 μ g/ μ l) or H-GP (10 μ g/ μ l) diluted in PBS immediately after LPS injection. Alternatively, dexamethasone (DXM) sodium phosphate at 10 μ g/ μ l (Shanghai General Motors Pharmaceutical Industry Company Limited, China) was injected as a positive control.

2.3.2. Clinical scoring

The EIU rats were examined using a biomicroscope 24 h after LPS injection. Clinical signs of EIU were graded from 0 to 4 in a blinded fashion according to a previously reported scoring system [17].

2.3.3. Number of infiltrating cells and protein concentration in the aqueous humor (AqH) from EIU rats

Twenty-four hours after LPS injection, the AqH was collected from the eyes immediately via an anterior chamber puncture using a 30-gauge needle. For cell counting, the AqH samples were suspended in Trypan-blue solution (1:5) and placed on a hemocytometer. The number of cells per field was manually counted under a light microscope (Olympus, Japan), and the number of cells per microliter was obtained by averaging the results of four fields from each sample. The total protein concentration in AqH was measured using a bicinchoninic acid (BCA) protein assay reagent kit (Pierce, Rockford, USA).

2.3.4. Concentrations of TNF- α and interleukin (IL)-6 in the AqH from EIU rats

The AqH from both eyes of each Wistar rat was centrifuged at 2500 rpm for 20 min at 4 $^{\circ}$ C. The levels of TNF- α and IL-6 in the AqH from EIU rats were determined using rat TNF- α and IL-6 ELISA kits (R&D Systems, Minneapolis, MN, USA), respectively, according to the manufacturer's instructions.

2.3.5. Histopathological examination

The eyeballs from the EIU rats (24 h after LPS injection) were enucleated and stored in a mixture of 10% formalin (Sinopharm Chemical Reagent Co., Ltd., Shanghai, China) and 2.5% glutaraldehyde (Sinopharm) for 24 h. For histopathological examination, tissue sections were deparaffinized using xylene (Sinopharm) and stained using hematoxylin and eosin (H&E; Sinopharm). Infiltrating leukocytes in the anterior chamber and vitreous cavity were counted, and the severity of inflammation was scored in a masked fashion as reported by Cousins [18].

2.4. Experimental autoimmune uveitis (EAU)

2.4.1. EAU induction and treatment

EAU was induced via an injection of 30 μ g R16 peptide emulsified in complete Freund's adjuvant (CFA; Sigma) containing 2.5 mg/ml killed *Mycobacterium tuberculosis* H37Ra (Difco, Detroit, MI, USA) into the left hind footpad of each Lewis rat. On days 6, 9 and 12, the Lewis rats were injected with PBS, H-RN, H-GP or DXM (all 10 μ g/ μ l) into both eyes.

2.4.2. Clinical scoring

For the EAU rats, each day after immunization, clinical signs were monitored and scored in a masked fashion using a grading scale from 0 to 4 as previously described by Agarwal and Caspi [19].

2.4.3. Levels of interferon (IFN)- γ and IL-6 in EAU rats

On day 14, after collection of the AqH, the iris ciliary body (ICB)-retina complex was isolated and placed in 100 μ l lysis buffer (Merek, Darmstadt, Germany) supplemented with protease inhibitors (Roche, Mannheim, Germany) and then sonicated. The lysate was centrifuged at 15,000 rpm for 10 min at 4 $^{\circ}$ C. The protein levels of IL-6 and IFN- γ were determined using ELISA kits (R&D).

2.4.4. Histopathological evaluation

All of the eyeballs from EAU rats (day 16 after immunization) were collected. Histopathologic scores of EAU were blindly determined using a scale from 0 to 4 according to the criteria of Agarwal and Caspi [19].

2.5. Cell culture

RAW264.7 murine macrophage cells, purchased from the Cell Bank of the Chinese Academic of Sciences (CBCAS, Shanghai, China), were cultured in Dulbecco's modified Eagle's medium (DMEM; Invitrogen-Gibco, Grand Island, NY, USA) supplemented with 10% fetal bovine serum (FBS; ScienCell, San Diego, CA, USA) and antibiotics (100 U/ml penicillin and 100 mg/ml streptomycin). Human umbilical vein endothelial cells (HUVECs, ScienCell) were maintained in endothelial cell culture media (ECM; ScienCell). U937 human monocyte-like cells were cultured in RPMI-1640 (Invitrogen-Gibco) supplemented with 10% FBS. The cells were maintained at 37 °C in an atmosphere containing 5% CO₂.

2.6. Cell viability assay

The cell viabilities of RAW264.7 cells and HUVECs were assessed using the Cell Titer 96 Aqueous One Solution Cell Proliferation (MTS) assay kit (Promega, Madison, WI, USA). In a 96-well plate, 5×10^4 /ml cells were seeded and serum-starved for 24 h, followed by treatment with various concentrations (50 to 500 μM) of peptides for another 24 h. The cells in the control group were untreated. Then, 20 μl of MTS reagent was added to each well, and the cells were incubated for another 3 h at 37 °C. The absorbance at 490 nm was measured using a microplate reader (Model 680, Bio-Rad, Hercules, CA, USA). The results are expressed as the percentage of the viability rate, calculated as (optical density of peptide treated sample/control sample) × 100%.

2.7. Levels of TNF-α and IL-6 in LPS-stimulated RAW264.7 cells

RAW264.7 cells were cultured in 24-well plates and starved in serum-free DMEM for 24 h. Then, the cells were treated with H-RN at various concentrations (50, 100 or 200 μM), H-GP (200 μM) or DXM (50 μM) for 30 min preceding the addition of LPS (100 ng/ml). The expression of TNF-α and IL-6 in the culture medium 24 h after LPS stimulation was assessed using ELISA kits (R&D).

The mRNA levels of TNF-α and IL-6 were assessed via RT-PCR analysis 6 h after LPS stimulation. Total RNA was extracted using Trizol reagent (Invitrogen) according to the manufacturer's instructions. Fluorescence quantitative RT-PCR was performed using a Rotor-Gene 3000 thermocycler (Corbett Research, Australia) with Realtime PCR Master Mix (TOYOBO Biotech, Japan) according to the protocol. β-Actin was chosen as the housekeeping gene. The specific sense and antisense primers used were: TNF-α, sense: 5'-CTGTAGCCACGTCGTAGC-3', anti-sense: 5'-TTGAGATC-CATGCCGTTG-3'; IL-6, sense: 5'-GACAACCTTGGCATTGTGG-3', anti-sense: 5'-ATGCAGGGATGATGTTCTG-3'; β-actin, sense: 5'-TGTGATGGTGGGAATGGGTACG-3', anti-sense: 5'-TTTGATGT-CACGCACGATTCC-3'.

2.8. Monocytic cell-endothelial cell adhesion assay

HUVECs (1.0×10^5 cells/well) were cultured in ECM containing 10% FBS in a 24-well plate. Once reaching 90% confluence, the cells were starved in serum-free ECM for 12 h and then treated with H-RN, H-GP or DXM for 18 h, followed by 6 h stimulation with TNF-α (10 ng/ml; PeproTech, USA). U937 cells were labeled with 10 μM CM-H2DCFDA (Invitrogen) in RPMI 1640 medium containing 10% FBS for 30 min. After three washes with PBS, the CM-H2DCFDA-labeled U937 cells were gently added to the HUVEC wells, and the cells were co-incubated at 37 °C for 60 min. The non-adherent U937 cells were then gently washed away using PBS containing 1% FBS and the HUVECs were fixed using 4% paraformaldehyde in PBS for 10 min, followed by a 20 min incubation at room temperature in rhodamine phalloidin (Molecular Probes, Eugene, Oregon, USA).

Random fields were imaged under a confocal laser scanning microscope (Zeiss LSM510; Carl Zeiss, Germany). The numbers of adherent U937 cells were counted in a masked fashion and expressed as the number of adherent cells per field.

2.9. Levels of P-selectin, E-selectin, ICAM-1 and VCAM-1 in TNF-α-stimulated HUVECs

HUVECs were cultured in 24-well plates and starved in serum-free DMEM for 24 h. Then, the cells were treated with H-RN at various concentrations (50, 100 or 200 μM), H-GP (200 μM) or DXM (50 μM) for 18 h followed by stimulation with TNF-α (10 ng/ml) for 6 h. The levels of P-selectin, E-selectin, ICAM-1 and VCAM-1 in the culture medium were assessed using a human adhesion molecule multiplex kit (R&D).

2.10. Transwell chemotaxis assay

Raw264.7 cells (3×10^5) pretreated for 30 min with H-RN (200 μM), H-GP (200 μM) or DXM (50 μM) were suspended in 300 μl of serum-free DMEM and overlaid onto transwell 8 μm pore filters in a 24-well plate format (Millipore, Bedford, MA, USA). The lower chambers contained serum-free DMEM with LPS (100 ng/ml). The control group was untreated. After incubation for 24 h, the cells were fixed and stained, and the non-migrating cells were removed from the upper surface using a cotton swab. The numbers of cells that passed through the filters were counted using a light microscope (Olympus).

2.11. Detection of FITC-labeled H-RN in RAW264.7 cells

RAW264.7 cells were cultured in glass-bottom dishes and starved in serum-free DMEM for 24 h. Then, the cells were treated with 200 μM FITC-labeled H-RN for 30 min, followed by stimulation with LPS (100 ng/ml). At 0.5 h, 6 h, 12 h or 24 h, the cells were fixed using 4% paraformaldehyde in PBS for 10 min and viewed under a confocal laser scanning microscope (Zeiss LSM510; Carl Zeiss).

2.12. Immunofluorescence staining of NF-κB p65 in RAW264.7 cells

Cells were seeded on cover slips to 70% confluence, pre-treated for 30 min with 200 μM H-RN and subsequently co-incubated with or without 100 ng/ml LPS. The cells were washed with PBS, fixed using 3.7% paraformaldehyde (Sigma) and permeabilized using 0.1% Triton X-100 (Promega) for 10 min. The slides were separately incubated overnight at 4 °C in a humidified chamber in antibodies against NF-κB p65 (Cell Signaling Technology, Beverly, MA, USA) or pp65^{Ser276} (Santa Cruz Biotechnology, CA, USA), followed the next day by a 1-h incubation at room temperature in the secondary antibody. The sections were stained using Hoechst 33342 (Invitrogen) for 5 min and then visualized and photographed under a confocal laser scanning microscope (Zeiss LSM510; Carl Zeiss). The number of translocated nuclei in six random fields were counted in a masked fashion and expressed as a percentage of the number of translocated cells relative to the total cells. The experiments were performed in triplicate and repeated at least three times.

2.13. Western blot

After treatment with various concentrations of H-RN (50, 100 or 200 μM) or H-GP (200 μM) in the presence or absence of LPS (100 ng/ml), whole cell extracts and nuclear extracts were prepared on ice. The protein concentrations were measured using the BCA assay (Pierce). The whole cell lysates and nuclear extracts

were separated via 10% SDS-PAGE and transferred to PVDF membranes. The membranes were blocked using 5% bovine serum albumin (BSA) and then incubated overnight 4 °C in primary antibodies against $\text{I}\kappa\text{B}\alpha$ (ABCAM, Cambridge, UK), PI3K-p85, phospho-p85^{Tyr458}, Akt, phospho-Akt^{Ser473}, phospho-IKK α/β , NF- κB -p65, PCNA (all from Cell Signaling Technology), IKK β , phospho-p65^{Ser276} or tubulin (all from Santa Cruz Biotechnology). Each membrane was then incubated in horseradish peroxidase (HRP)-conjugated secondary antibodies (Santa Cruz Biotechnology) for 1 h. The bands were visualized using the ECL detection system (Pierce), and the band density was determined using ImageJ software (National Institutes of Health (NIH), USA).

2.14. Statistical analysis

The data are expressed as the means \pm SD of at least three independent experiments. The differences between mean values of multiple groups were analyzed via one-way ANOVA with Bonferroni post hoc analysis, and the Mann–Whitney *U*-test was used for non-parametric data analysis. A *p*-value <0.05 was considered to be

statistically significant. All computations were performed using SPSS17.0 (Chicago, IL, USA) software.

3. Results

3.1. Anti-inflammatory effects of H-RN in EIU rats

3.1.1. H-RN suppressed the clinical score, the protein concentration and the number of cells in the AqH of EIU rats

Twenty-four hours after LPS injection, severe inflammation was detected in the anterior chamber, and the clinical score for the EIU rats treated with PBS was 3.40 ± 0.52 . H-RN treatment reduced the inflammation and improved the clinical score in a dose-dependent manner. After intravitreal injection of $10 \mu\text{g}/\mu\text{l}$ H-RN, none of the eyes were scored as 4, and the clinical score was significantly reduced to 1.70 ± 0.68 . This effect was comparable to the positive control group, which received DXM treatment (Fig. 2A and B). H-RN administration also decreased the protein concentration in a dose-dependent manner (Fig. 2C). Likewise, the number of inflammatory cells in the AqH was significantly decreased in the groups treated with

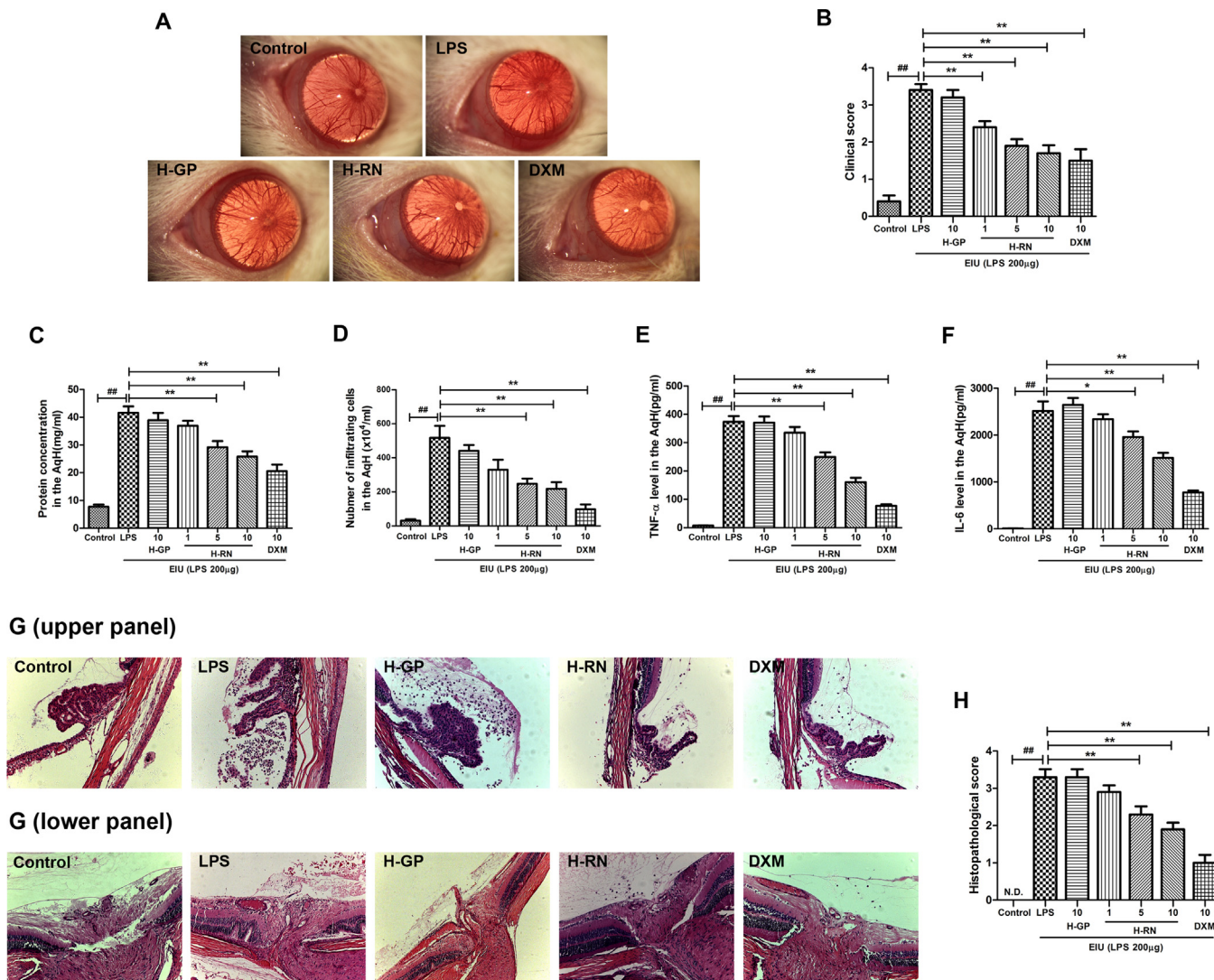


Fig. 2. Anti-inflammatory effects of H-RN in EIU rats. Wistar rats were treated intravitreally with PBS, H-GP ($10 \mu\text{g}/\mu\text{l}$), H-RN ($1, 5, 10 \mu\text{g}/\mu\text{l}$) or DXM ($10 \mu\text{g}/\mu\text{l}$) in both eyes immediately after LPS induction. Clinical manifestations were evaluated under a biomicroscope (A) and scored in a blinded fashion (B) 24 h after LPS injection. Effects of H-RN, H-GP and DXM on protein concentration (C), infiltrating cell numbers (D), levels of TNF- α (E) and IL-6 (F) in AqH of EIU rats were assessed. EIU rats' eyeballs were fixed, sectioned and stained with H&E 24 h after LPS stimulation. Inflammatory cell infiltration was evaluated in the ICB region ((G), upper panel) and posterior vitreous and retina ((G), lower panel), original magnification $\times 100$. The severity of inflammation was scored in a masked fashion (H). Data are expressed as mean \pm SD ($n = 10$ per group). ## $p < 0.01$ compared to the control group; ** $p < 0.01$ compared to the PBS-treated group. N.D., Not detected.

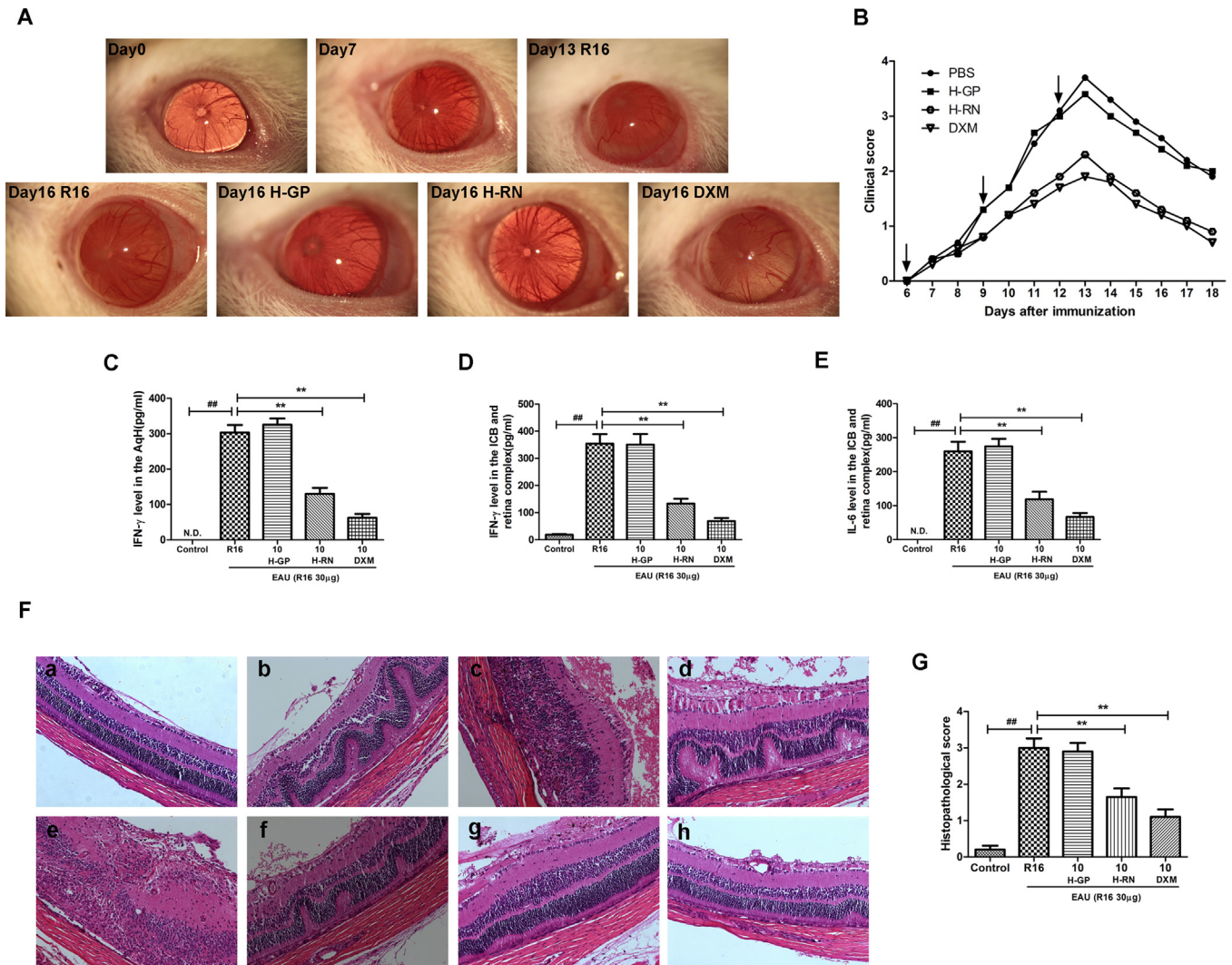


Fig. 3. Anti-inflammatory effects of H-RN in EAU rats. Lewis rats were immunized by injection of 30 μ g R16 peptide emulsified in complete Freund's adjuvant containing 2.5 mg/ml killed Mycobacterium tuberculosis into the left hind footpads. On day 6, 9 and 12, Lewis rats were intravitreally treated with PBS, H-RN, H-GP or DXM (all 10 μ g/ μ l) in both eyes. Each day after immunization, clinical signs were monitored (A) and scored in a masked fashion (B), note the black arrows: H-RN injection). On day 14, IFN- γ levels in the AqH (C) and ICB-retina complex (D) as well as IL-6 level in the ICB-retina complex (E) were assessed. On day 16, histopathologic sections were evaluated. (F) Representative histopathology of EAU rats, original magnification, \times 200. (a) The retina of a normal rat; ((b) and (c)) PBS-treated; ((d) and (e)) H-GP-treated; ((f) and (g)) H-RN-treated; (h) DXM-treated. (H) Histopathologic scores were assigned blindly. Data are expressed as mean \pm SD ($n = 8$ per group). $^{##} p < 0.01$ compared to the control group; $^{**} p < 0.01$ compared to the PBS-treated group. N.D., Not detected.

H-RN or DXM (Fig. 2D). However, intravitreal injection of H-GP had no therapeutic effect on EIU ocular inflammation.

3.1.2. H-RN decreased TNF- α and IL-6 expression in the AqH from EIU rats

The TNF- α and IL-6 levels were remarkable 24 h after LPS stimulation (TNF- α : 373.6 ± 63.46 pg/ml; IL-6: 2513 ± 651.97 pg/ml). Treatment with 5 μ g/ μ l H-RN significantly reduced the secretion of TNF- α and IL-6, and a stronger effect was exhibited when the rats were treated with 10 μ g/ μ l H-RN or DXM. Meanwhile, no effect was detected in the EIU rats treated with 10 μ g/ μ l H-GP (Fig. 2E and F).

3.1.3. Histopathological changes in EIU rats

Histological evaluation revealed severe cellular infiltration in the anterior chamber, the ICB and the posterior vitreous cavity 24 h after LPS injection. No inflammation was detected histopathologically in the control group. The number of inflammatory cells in the ICB and the posterior vitreous was significantly decreased in the H-RN- and DXM-treated eyes. However, treatment with H-GP did not induce any decrease in inflammation (Fig. 2G and H).

3.2. Anti-inflammatory effects of H-RN in EAU rats

3.2.1. H-RN suppressed the clinical score of EAU rats

The therapeutic effect of H-RN on EAU in the anterior segment was assessed via clinical scoring. Lewis rats immunized with R16 exhibited ocular inflammation beginning on day 7 and peaking around day 13. The rats treated with 10 μ g/ μ l H-RN and DXM exhibited a significant reduction in clinical scores beginning on day 11, while those treated with H-GP exhibited no anti-inflammatory effect. However, approximately 30% of the eyes treated with DXM developed a moderate to severe cataract approximately two weeks after immunization, while the H-RN- and H-GP-treated rats exhibited less frequent and milder manifestation (Fig. 3A and B).

3.2.2. H-RN inhibited the production of IL-6 and IFN- γ in EAU rats

Significantly lower levels of IFN- γ in both the AqH and the ICB-retina complex and IL-6 in the ICB-retina complex were detected in the H-RN and DXM groups compared to the PBS and H-GP groups (Fig. 3C–E). The level of IL-6 in the AqH from EAU rats was too low to generate meaningful statistical analyses.

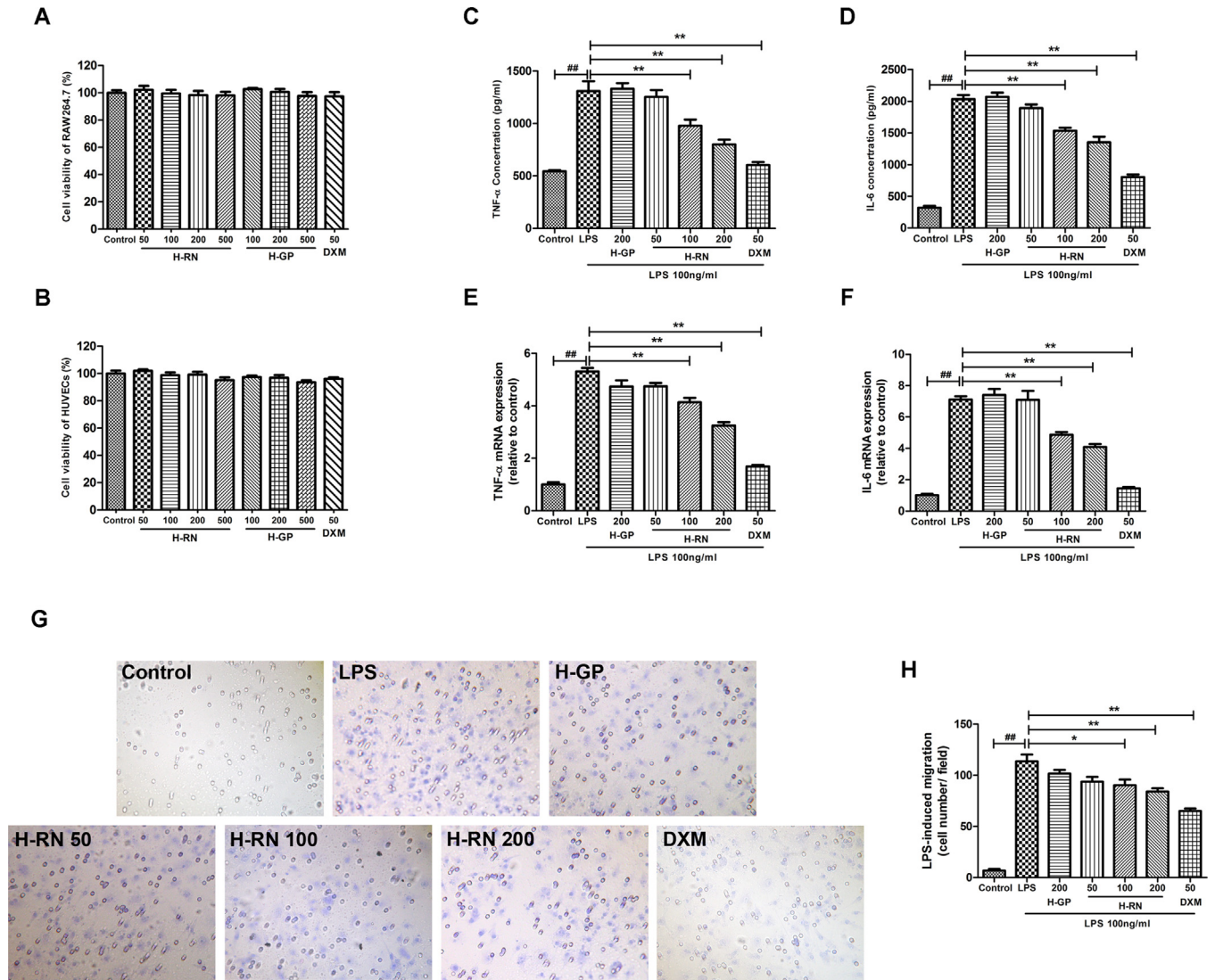


Fig. 4. Effects of H-RN on LPS-stimulated TNF- α and IL-6 production and chemotaxis of RAW 264.7 cells. The MTS assay suggested that cell viability of RAW264.7 cells (A) and HUVECs (B) did not show any variation after incubation with H-RN or H-GP at various concentrations (up to 500 μ M) for 24 h. RAW 264.7 cells were treated with (50, 100, 200 μ M), H-GP (200 μ M) or DXM (50 μ M) for 30 min before 24 h-combined incubation with LPS (100 ng/ml). The protein expression of TNF- α and IL-6 were assessed by ELISA ((C) and (D)) while mRNA levels were quantified by real-time PCR and normalized to β -actin mRNA level ((E) and (F)). The chemotaxis of RAW 264.7 cells toward LPS were assessed with a transwell filter (G). Quantification of chemotactic migrating is presented by the migrated cells per field counted (H). All samples were analyzed in duplicate and repeated at least three times. Data are expressed as mean \pm SD. ## $p < 0.01$ compared to the control group; * $p < 0.05$, and ** $p < 0.01$ compared to the LPS group.

3.2.3. Histopathological evaluation of the EAU rats

Severe inflammatory cell infiltration and photoreceptor destruction was detected in the rats treated with PBS (Fig. 3F(b and c)) and H-GP (Fig. 3F(d and e)), with scores of 3.0 ± 0.8 and 2.9 ± 0.7 , respectively. A significant improvement was found in both H-RN (1.65 ± 0.7 , Fig. 3F(f and g)) and DXM-treated (1.1 ± 0.6 , Fig. 3F(h)) rats, exhibiting mild to moderate cell infiltration and retina destruction.

3.3. H-RN and H-GP are non-toxic to RAW264.7 cells and HUVECs

The viability of RAW264.7 cells and HUVECs did not display any variation after incubation in H-RN at various concentrations (50, 100, 200 or 500 μ M) or H-GP (100, 200 or 500 μ M) for 24 h based on the MTS cytotoxicity assay (Fig. 4A and B).

3.4. H-RN suppressed the LPS-induced expression of TNF- α and IL-6 in RAW264.7 cells

TNF- α and IL-6 are known to be important inflammatory cytokines associated with LPS stimulation [20]. After co-treatment

with various doses of H-RN (50, 100 or 200 μ M) and LPS (100 ng/ml) for 24 h, suppression of the LPS-induced expression of TNF- α and IL-6 was detected in a dose-dependent manner at both the protein (Fig. 4C and D) and the transcriptional level (Fig. 4E and F).

3.5. H-RN attenuated the chemotaxis of RAW264.7 cells toward LPS

As shown in Fig. 4G and H, the number of RAW 264.7 cells chemotactic migrating toward LPS was reduced by pretreatment with 200 μ M H-RN, although its inhibitory effect was not as strong as that of 50 μ M DXM. In contrast, the cells pretreated with H-GP did not display a significant difference compared to LPS treatment alone.

3.6. H-RN inhibited the adhesion of U937 cells to TNF- α -stimulated HUVECs

The effect of H-RN on the adhesion of U937 cells to TNF- α -activated endothelial cells, a critical step in vascular inflammation, was also investigated. As shown in Fig. 5A and B, non-stimulated HUVECs displayed minimal binding to U937 cells, while stimulation

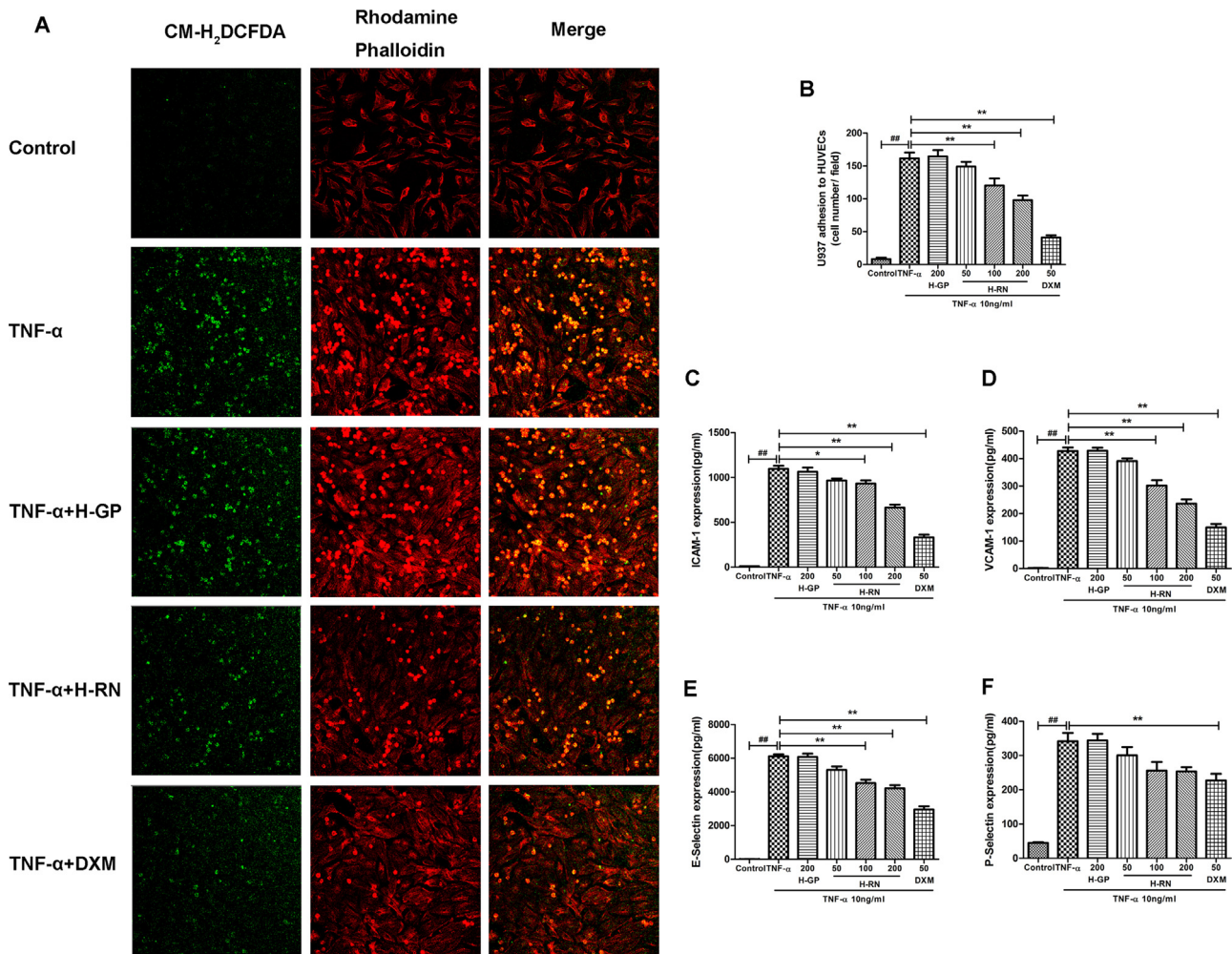


Fig. 5. Effects of H-RN on TNF- α -stimulated monocyte-endothelial cell adhesion and expression of adhesion molecules in HUVECs. (A) HUVECs were incubated with H-RN (50, 100, 200 μ M), H-GP (200 μ M) or DXM (200 μ M) for 18 h, followed by 6 h stimulation with TNF- α (10 ng/ml). U937 cells labeled with CM-H2DCFDA (green fluorescence) were seeded onto HUVECs and co-cultured for 60 min. After removing the non-adherent cells, adherent cells were fixed and stained with rhodamine phalloidin (red fluorescence). Random fields were imaged under a confocal laser scanning microscopy, original magnification $\times 200$. (B) Quantification of monocyte adhesion is presented by the number of adhered U937 cells per field counted. Effects of H-RN on levels of ICAM-1 (C), VCAM-1 (D), E-selectin (E) and P-selectin (F) in TNF- α -stimulated HUVECs were determined with a human adhesion molecule multiplex kit. Data are expressed as mean \pm SD of results from three independent experiments, each performed in duplicate. ## $p < 0.01$ compared to the control group; * $p < 0.05$, and ** $p < 0.01$ compared to the TNF- α group. (For interpretation of the references to color in this figure legend, the reader is referred to the web version of this article.)

of HUVECs with TNF- α for 6 h resulted in significant an increase in adherent U937 cells. Meanwhile, the adhesion of U937 cells to TNF- α -stimulated HUVECs was significantly attenuated by 200 μ M H-RN, while a stronger inhibitory effect was detected upon pretreatment with 50 μ M DXM. H-GP did not display any effect on the adhesion of U937 cells to HUVECs (Fig. 5A and B).

3.7. H-RN inhibited the TNF- α -stimulated expression of P-selectin, E-selectin, ICAM-1 and VCAM-1 in HUVECs

TNF- α is recognized as a major risk factor that promotes endothelial dysfunction by enhancing the expression of adhesion molecules on endothelial cells during the inflammation process [21]. We investigated the effect of H-RN on TNF- α -stimulated adhesion molecule expression using a human adhesion molecule multiplex kit. The results revealed that the levels of adhesion molecules were very low in non-stimulated HUVECs but were significantly increased by TNF- α stimulation. Treatment with 50 μ M DXM significantly suppressed TNF- α -induced adhesion molecule expression. TNF- α -induced ICAM-1, VCAM-1 and E-selectin expression was inhibited by H-RN in a dose-concentration manner at concentrations ranging from 50 to 200 μ M, while no

suppression of P-selectin expression was detected. Pretreatment with 200 μ M H-GP displayed no apparent reduction in TNF- α -induced adhesion molecule expression (Fig. 5C–F).

3.8. Determination of the localization of H-RN in RAW264.7 cells

We investigated the localization of H-RN in RAW264.7 cells by viewing FITC-labeled H-RN via confocal microscopy. After stimulation with LPS for 0.5 h, the FITC-labeled H-RN began to touch and enter the RAW cells, while at 6 h after LPS stimulation, more FITC-labeled H-RN was found to be enclosed in phagosome-like structure predominantly in the cytoplasm of the cells. After 12 h, a similar phenomenon was observed, but some H-RN had translocated near the nuclear membrane. After 24 h, we found some FITC inside the nucleus (Fig. 6A). Thus, we speculated that H-RN enters the cells via phagocytosis and partially localizes near or in the nucleus.

3.9. H-RN inhibited the activation of NF- κ B p65 in LPS-stimulated RAW264.7 cells

The phosphorylation and translocation of the NF- κ B p65 subunit, a marker of NF- κ B activation, plays an important role

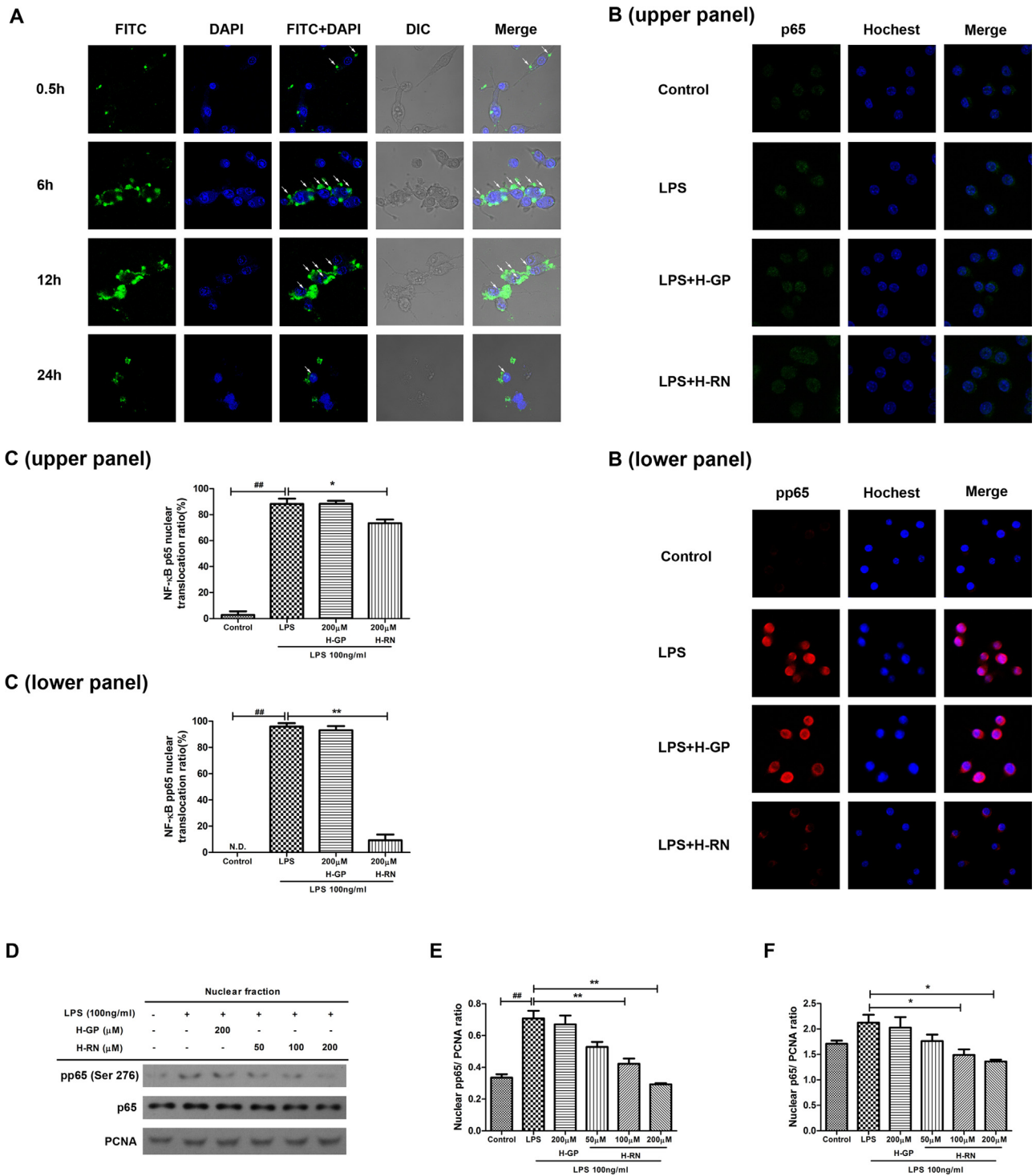


Fig. 6. (A) Determination of the localization of H-RN in RAW264.7 cells. With stimulation of LPS for 0.5 h, the FITC-labeled H-RN (green fluorescence) started to touch and began to enter cells. After 6 h, more FITC-labeled H-RN was found to be enclosed in phagosome-like structure predominantly in the cytoplasm of the cells (white arrows). After 12 h, besides the fluorescence observed in the cytoplasm, some H-RN had translocated near the nuclear membrane (white arrows). After 24 h, some fluorescein was observed inside the nucleus (white arrows). (B) Effects of H-RN on NF-κB activity in LPS-stimulated RAW264.7 cells. The intracellular locations of NF-κB p65 and pp65 were assessed by immunofluorescence using secondary antibodies labeled with FITC (green fluorescence, upper panel) or with rhodamine (red fluorescence, lower panel), and the nuclei were stained with Hoechst 33342 (blue fluorescence). (C) The number of nuclear activated cells in six random fields were counted in a masked fashion and expressed as a percentage of the number of activated cells in comparison to total cells. (D) Cells were pretreated with H-RN (50, 100, 200 μM) or H-GP (200 μM) for 30 min and then stimulated with 100 ng/ml LPS for 1 h. Nuclear proteins were analyzed by western blot analysis using antibody against NF-κB p65 or pp65. PCNA was used as the internal control. The band density was determined by Image J software and the relative level was calculated as the ratio of NF-κB p65 (E) or pp65 (F) to PCNA protein expression. The results represent means ± S.D. Experiments were performed in triplicate and repeated at least three times. ^{##} $p < 0.01$ compared to the control group; ^{*} $p < 0.05$, and ^{**} $p < 0.01$ compared to the LPS group. (For interpretation of the references to color in this figure legend, the reader is referred to the web version of this article.)

in regulating the expression of various genes encoding pro-inflammatory cytokines and adhesion molecules. We found that pretreatment with 200 μ M H-RN exhibited mild to moderate inhibition of the LPS-activated nuclear translocation of p65 and significantly attenuated the phospho-p65 level inside the nucleus (Fig. 6B and C). As shown in Fig. 6D and E, quantitative analysis revealed a significant increase in the expression of phospho-p65 inside the nucleus in LPS-stimulated RAW264.7 cells, while the level of phospho-p65 decreased in the H-RN-treated group in a dose-dependent manner ranging from 50 to 200 μ M.

3.10. H-RN inhibited LPS-induced $I\kappa$ B α degradation and activation of the PI3K-AKT-IKK signaling pathway

After LPS-induced $I\kappa$ B α -degradation, phosphorylation of p65 at Ser276 is activated in the cytoplasm. This phosphorylation is thought to break an intramolecular interaction between the C-terminal region of the protein and the Rel homology domain, thereby facilitating DNA binding and interaction with the transcriptional co-activators p300 and cAMP response element-binding (CREB)-binding protein (CBP). Western blot analysis revealed that H-RN inhibited LPS-induced $I\kappa$ B α degradation (Fig. 7E). We also explored the upstream mechanisms of the PI3K-AKT-IKK pathway, a major regulator of NF- κ B. The results revealed that H-RN pretreatment concentration-dependently suppressed the phosphorylation level of p85 (Fig. 7B) and AKT (Fig. 7C) in LPS-stimulated RAW 264.7 cells, which was consistent with its inhibitory effect on the IKK α / β phosphorylation level (Fig. 7D). These results suggested that H-RN may inhibit LPS-induced inflammation by influencing the PI3K/AKT/IKK/NF- κ B pathway.

4. Discussion

For ocular inflammatory diseases, including uveitis, traditional treatments such as corticosteroids and immunosuppressive agents

can cause multiple adverse effects [22–24]. Due to these side-effects, investigators have attempted to develop new alternatives. Several existing drugs are being assessed, including anti-VEGF compounds, such as ranibizumab [25] and bevacizumab [26,27], and anti-TNF- α antibodies [28,29]. Furthermore, the advent of biotechnology is stimulating advances in the generation of new therapeutic molecules, such as high affinity binding peptides or modified high affinity or bivalent single chain Fab fragments, offering higher specificity and the possibility of topical delivery [30]. Compared with proteins, peptides display lower immunogenicity, higher solubility in water, more stable production methods, improved consistency between batches and superior targeting and penetration [31].

First, our in vitro and in vivo results suggest that H-RN can inhibit inflammation, while the scrambled peptide H-GP displayed no effect, which indicates that the unique sequence of the H-RN peptide is responsible for its biological function.

The EIU and EAU models are widely accepted animal models to assess the pharmacological and immunological effects of drugs on intraocular inflammation. EIU is induced via a single stimulation of a sublethal dose of LPS in the footpad [32], and it is suitable for the evaluation of the therapeutic efficacy of drugs for the treatment of acute human inflammatory ocular diseases [33]. We found that H-RN significantly ameliorated the severity of protein transudation in the anterior chamber, infiltration of inflammatory cells into the eye and production of proinflammatory mediators, such as TNF- α and IL-6, in EIU rats 24 h after intravitreal injection.

On the other hand, chronic intraocular inflammation is induced using a prolonged and severe stimulus in EAU rats. We investigated the clinical and histopathological effects of H-RN administered every 3 days beginning on day 6 after inoculation, and significant immunosuppressive effects were found beginning on day 11 and lasted for at least 7 days. IFN- γ , an important cytokine produced by T helper 1 (Th1) cells, was effectively suppressed by H-RN in both the AqH and the ICB-retina complex. Moreover, H-RN attenuated

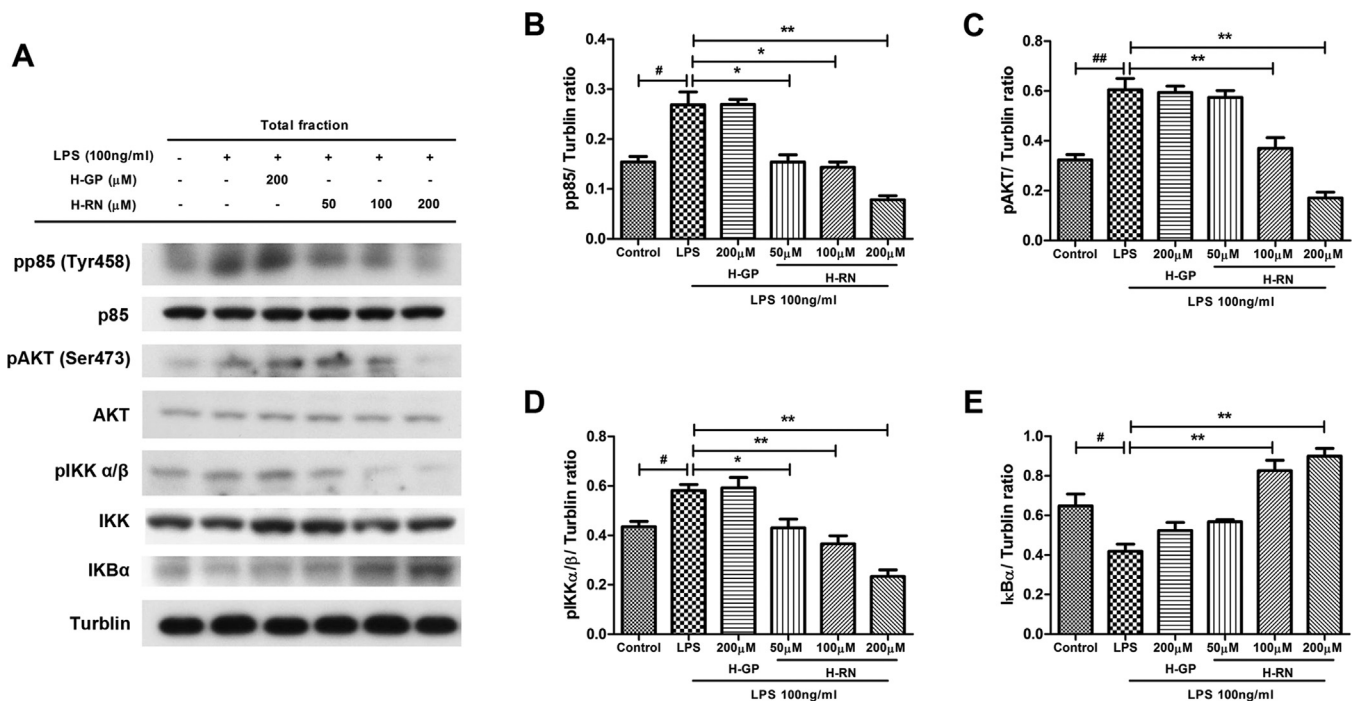


Fig. 7. Effects of H-RN on PI3K/AKT/IKK signal pathway. (A) RAW 264.7 cells were pretreated with H-RN (50, 100, 200 μ M) or H-GP (200 μ M) for 30 min and then stimulated with 100 ng/ml LPS for 1 h. The expression levels of pp85, p85 pAKT^{Ser473}, AKT, pIKK α / β , IKK or $I\kappa$ B α in whole cell extract were assessed by Western blotting. Turblin was used as the internal control. The band density was determined by Image J software and the relative level was calculated as the ratio of pp85 (B), pAKT (C), pIKK α / β (D) or $I\kappa$ B α (E) to Turblin expression. The results represent means \pm S.D. Experiments were performed in triplicate and repeated at least three times. # $p < 0.05$, and ## $p < 0.01$ compared to the control group; * $p < 0.05$, and ** $p < 0.01$ compared to the LPS group.

IL-6 expression, which is also one of the key proinflammatory cytokines produced in EAU pathogenesis and plays an important role in Th17 differentiation [34]. However, the effects of different modes of administration, as well as the anti-inflammatory mechanisms of H-RN in EIU and EAU models, require further study.

Macrophages play a crucial role in the inflammatory and immune responses by recognizing and phagocytizing pathogens, secreting cytokines and chemokines, processing antigens and repairing tissue damage [35]. LPS can activate macrophages and initiate inflammatory and immune responses, which induces the production of inflammatory cytokines, including TNF- α and IL-6, which are biomarkers of inflammation [36,37]. In our study, we found that H-RN suppressed LPS-stimulated TNF- α and IL-6 expression at both the protein and mRNA levels in RAW 264.7 cells, and this result was consistent with the anti-inflammatory effect of H-RN in the LPS-induced EIU model. Moreover, H-RN inhibited the chemotaxis of RAW264.7 cells toward LPS, which is another key event in the recruitment of leukocytes during inflammation.

We also demonstrated that H-RN attenuated TNF- α -induced adhesion molecule expression in HUVECs, including ICAM-1, VCAM-1 and E-selectin. These molecules are also essential for the migration and adhesion of inflammatory cells. This inhibition contributed to the suppressive effect of H-RN on the adhesion of U937 cells to endothelial cells. Our finding is in agreement with previous reports that HGF, the source protein of H-RN, significantly diminished the adhesion of monocytes to a TNF-activated endothelial monolayer [38,39].

NF- κ B is a ubiquitous transcription factor that is important for the response to a wide variety of pro-inflammatory stimuli. This nuclear factor exists in an inactive form, and its activation involves the rapid phosphorylation of I κ B by the IKK complex. The free p65 protein then translocates to the nucleus, binds to target genes and affects the transcription of pro-inflammatory mediators [40]. We demonstrated effects of H-RN on the PI3K/Akt pathway and NF- κ B activation, which is responsible for the anti-inflammatory effect of HGF [41]. The results suggested that H-RN entered the cells via phagocytosis and inhibited the PI3K p85 subunit and AKT phosphorylation, which may result in the attenuation of LPS-induced IKK complex activation and I κ B degradation, which leads to NF- κ B activation. As reported, Ser276 is phosphorylated by protein kinase A (PKA) in the cytoplasm and mitogen- and stress activated protein kinase (MAK)-1 and MAK-2 in the nucleus [42]. Based on our western blot results, the inhibition of nuclear phospho-p65 expression by H-RN was especially notable, indicating that the inhibitory effect of H-RN on p65 phosphorylation may also occur inside the nucleus. Interestingly, the significant anti-phosphorylation effect of H-RN at Ser276 of p65 led us to hypothesize that H-RN possibly mediates the crosstalk between the ERK and p38 MAPK pathways, as MAPKs also play an important role in inducing LPS-stimulated cytokine production [43–45]. However, the activation of MAPKs and their interactions with the NF- κ B pathway require future studies.

Although the anti-inflammatory effect of H-RN is not as strong as that of DXM, its advantages with respect to ocular safety and simple synthesis make it a potential candidate for therapeutic intervention for inflammation. When combined with other drugs, H-RN may offer more alternatives to ocular diseases. For instance, combined with intraocular pressure-lowering drugs, H-RN may contribute to the treatment of neovascular glaucoma since it exhibits both anti-inflammatory and anti-neovascular effects. Additionally, in patients post corneal transplantation, H-RN may inhibit ocular inflammation as well as prevent neovascularization and provide a combination choice with immunosuppressants. Moreover, H-RN can partially replace the use of glucocorticoids in chronic uveitis to decrease the potential side-effects.

One of the major limitations of peptides in clinical applications is their short half-life and the necessity of repeated treatment. Chemical modification and conjugation would be helpful. It would also be greatly practicable to develop a drug-release system for peptides to enhance its localization at the target site and to sustain the drug concentration. In addition, the inhibitory activity of H-RN on ocular surface inflammation, such as keratitis and conjunctivitis, using a formulation of eye drops is also under examination.

In conclusion, our results demonstrated that intravitreal injection of H-RN, an antiangiogenic peptide derived from HGF K1, can inhibit inflammation in EIU and EAU clinically and histopathologically. Meanwhile, H-RN suppressed inflammatory cytokine production, as well as the adhesion and migration of inflammatory cells, possibly by interfering with the PI3K-AKT-IKK-I κ B-NF- κ B signaling pathway. Considering its advantages with respect to ocular safety and simple synthesis, H-RN may provide a promising candidate for ocular anti-inflammation therapy.

Acknowledgments

This work was supported by National Natural Science Foundation of China nos. 81273424, 81170862 and 81300753, and National Science and Technology Major Project (2011ZX09302-007-02). The authors also thank Li Su, Xiaolu Yang, Huiyi Jin, Mingming Ma for excellent technical assistance throughout the project.

References

- [1] Chang JH, Wakefield D. Uveitis: a global perspective. *Ocul Immunol Inflamm* 2002;10:263–79.
- [2] Suhler EB, Lloyd MJ, Choi D, Rosenbaum JT, Austin DF. Incidence and prevalence of uveitis in Veterans Affairs Medical Centers of the Pacific Northwest. *Am J Ophthalmol* 2008;146:890–6. e8.
- [3] Folkman J. Angiogenesis in cancer, vascular, rheumatoid and other disease. *Nat Med* 1995;1:27–31.
- [4] Carmeliet P. Angiogenesis in health and disease. *Nat Med* 2003;9:653–60.
- [5] Rajashekhar G, Willuweit A, Patterson CE, Sun P, Hilbig A, Breier G, et al. Continuous endothelial cell activation increases angiogenesis: evidence for the direct role of endothelium linking angiogenesis and inflammation. *J Vasc Res* 2006;43:193–204.
- [6] Fiedler U, Reiss Y, Scharpfenecker M, Grunow V, Koidl S, Thurston G, et al. Angiopoietin-2 sensitizes endothelial cells to TNF-alpha and has a crucial role in the induction of inflammation. *Nat Med* 2006;12:235–9.
- [7] Boulton M. A role for hepatocyte growth factor in diabetic retinopathy. *Br J Ophthalmol* 1999;83:763–4.
- [8] Colombo ES, Menicucci G, McGuire PG, Das A. Hepatocyte growth factor/scatter factor promotes retinal angiogenesis through increased urokinase expression. *Invest Ophthalmol Vis Sci* 2007;48:1793–800.
- [9] Gong R. Multi-target anti-inflammatory action of hepatocyte growth factor. *Curr Opin Invest Drugs* 2008;9:1163–70.
- [10] Shen Z, Yang ZF, Gao Y, Li JC, Chen HX, Liu CC, et al. The kringle 1 domain of hepatocyte growth factor has antiangiogenic and antitumor cell effects on hepatocellular carcinoma. *Cancer Res* 2008;68:404–14.
- [11] Lu Q, Zhang L, Shen X, Zhu Y, Zhang Q, Zhou Q, et al. A novel and effective human hepatocyte growth factor kringle 1 domain inhibits ocular neovascularization. *Exp Eye Res* 2012;105:15–20.
- [12] Chang PC, Wu HL, Lin HC, Wang KC, Shi GY. Human plasminogen kringle 1–5 reduces atherosclerosis and neointima formation in mice by suppressing the inflammatory signaling pathway. *J Thromb Haemost* 2010;8:194–201.
- [13] Jin J, Zhou KK, Park K, Hu Y, Xu X, Zheng Z, et al. Anti-inflammatory and antiangiogenic effects of nanoparticle-mediated delivery of a natural angiogenic inhibitor. *Invest Ophthalmol Vis Sci* 2011;52:6230–7.
- [14] Chavakis T, Athanasopoulos A, Rhee JS, Orlova V, Schmidt-Woll T, Bierhaus A, et al. Angiostatin is a novel anti-inflammatory factor by inhibiting leukocyte recruitment. *Blood* 2005;105:1036–43.
- [15] Xu Y, Zhao H, Zheng Y, Gu Q, Ma J, Xu X. A novel antiangiogenic peptide derived from hepatocyte growth factor inhibits neovascularization in vitro and in vivo. *Mol Vis* 2010;16:1982–95.
- [16] Sun Y, Su L, Wang Z, Xu Y, Xu X. H-RN, a peptide derived from hepatocyte growth factor, inhibits corneal neovascularization by inducing endothelial apoptosis and arresting the cell cycle. *BMC Cell Biol* 2013;14:8.
- [17] Behar-Cohen FF, Savoldelli M, Parel JM, Goureau O, Thillaye-Goldenberg B, Courtois Y, et al. Reduction of corneal edema in endotoxin-induced uveitis after application of L-NAME as nitric oxide synthase inhibitor in rats by iontophoresis. *Invest Ophthalmol Vis Sci* 1998;39:897–904.
- [18] Cousins SW, Guss RB, Howes Jr EL, Rosenbaum JT. Endotoxin-induced uveitis in the rat: observations on altered vascular permeability, clinical findings, and histology. *Exp Eye Res* 1984;39:665–76.

- [19] Agarwal RK, Caspi RR. Rodent models of experimental autoimmune uveitis. *Methods Mol Med* 2004;102:395–419.
- [20] Raetz CR, Whitfield C. Lipopolysaccharide endotoxins. *Annu Rev Biochem* 2002;71:635–700.
- [21] Yang WS, Lee JM, Han NJ, Kim YJ, Chang JW, Park SK. Mycophenolic acid attenuates tumor necrosis factor- α -induced endothelin-1 production in human aortic endothelial cells. *Atherosclerosis* 2010;211:48–54.
- [22] Tellier Z. Human immunoglobulins in intraocular inflammation. *Ann NY Acad Sci* 2007;1110:337–47.
- [23] Urtti A. Challenges and obstacles of ocular pharmacokinetics and drug delivery. *Adv Drug Deliv Rev* 2006;58:1131–5.
- [24] Samudre SS, Lattanzio Jr FA, Williams PB, Sheppard Jr JD. Comparison of topical steroids for acute anterior uveitis. *J Ocul Pharmacol Ther* 2004;20:533–47.
- [25] Acharya NR, Hong KC, Lee SM. Ranibizumab for refractory uveitis-related macular edema. *Am J Ophthalmol* 2009;148:303–9. e2.
- [26] Cordero Coma M, Sobrin L, Onal S, Christen W, Foster CS. Intravitreal bevacizumab for treatment of uveitic macular edema. *Ophthalmology* 2007;114:1574–9. e1.
- [27] Mackensen F, Heinz C, Becker MD, Heiligenhaus A. Intravitreal bevacizumab (avastin) as a treatment for refractory macular edema in patients with uveitis: a pilot study. *Retina* 2008;28:41–5.
- [28] Sfikakis PP, Theodossiadis PG, Katsiari CG, Kaklamanis P, Markomichelakis NN. Effect of infliximab on sight-threatening panuveitis in Behcet's disease. *Lancet* 2001;358:295–6.
- [29] Theodossiadis PG, Markomichelakis NN, Sfikakis PP. Tumor necrosis factor antagonists: preliminary evidence for an emerging approach in the treatment of ocular inflammation. *Retina* 2007;27:399–413.
- [30] Tempest-Roe S, Joshi L, Dick AD, Taylor SR. Local therapies for inflammatory eye disease in translation: past, present and future. *BMC Ophthalmol* 2013;13:39.
- [31] Sulochana KN, Ge R. Developing antiangiogenic peptide drugs for angiogenesis-related diseases. *Curr Pharm Des* 2007;13:2074–86.
- [32] Bhattacherjee P, Williams RN, Eakins KE. An evaluation of ocular inflammation following the injection of bacterial endotoxin into the rat foot pad. *Invest Ophthalmol Vis Sci* 1983;24:196–202.
- [33] Rosenbaum JT, McDevitt HO, Guss RB, Egbert PR. Endotoxin-induced uveitis in rats as a model for human disease. *Nature* 1980;286:611–3.
- [34] Horai R, Caspi RR. Cytokines in autoimmune uveitis. *J Interferon Cytokine Res* 2011;31:733–44.
- [35] Herrero C, Sebastian C, Marques L, Comalada M, Xaus J, Valledor AF, et al. Immunosenescence of macrophages: reduced MHC class II gene expression. *Exp Gerontol* 2002;37:389–94.
- [36] Dziarski R, Gupta D. Role of MD-2 in TLR2- and TLR4-mediated recognition of Gram-negative and Gram-positive bacteria and activation of chemokine genes. *J Endotoxin Res* 2000;6:401–5.
- [37] Wang Z, Jiang W, Zhang Z, Qian M, Du B. Nitidine chloride inhibits LPS-induced inflammatory cytokines production via MAPK and NF- κ B pathway in RAW 264.7 cells. *J Ethnopharmacol* 2012;144:145–50.
- [38] Gong R, Rifai A, Dworkin LD. Hepatocyte growth factor suppresses acute renal inflammation by inhibition of endothelial E-selectin. *Kidney Int* 2006;69:1166–74.
- [39] Gong R, Rifai A, Dworkin LD. Anti-inflammatory effect of hepatocyte growth factor in chronic kidney disease: targeting the inflamed vascular endothelium. *J Am Soc Nephrol* 2006;17:2464–73.
- [40] Siebenlist U, Franzoso G, Brown K. Structure, regulation and function of NF- κ B. *Annu Rev Cell Biol* 1994;10:405–55.
- [41] Boros P, Miller CM. Hepatocyte growth factor: a multifunctional cytokine. *Lancet* 1995;345:293–5.
- [42] Oeckinghaus A, Ghosh S. The NF- κ B family of transcription factors and its regulation. *Cold Spring Harbor Perspect Biol* 2009;1:a000034.
- [43] Rao KM. MAP kinase activation in macrophages. *J Leukoc Biol* 2001;69:3–10.
- [44] Perkins ND. Integrating cell-signalling pathways with NF- κ B and IKK function. *Nat Rev Mol Cell Biol* 2007;8:49–62.
- [45] Vermeulen L, De Wilde G, Van Damme P, Vanden Berghe W, Haegeman G. Transcriptional activation of the NF- κ B p65 subunit by mitogen- and stress-activated protein kinase-1 (MSK1). *EMBO J* 2003;22:1313–24.